Energy Storage and Strain-Recovery Processes in Highly Deformed Semicrystalline Poly(butylene terephthalate)

T. RICCO, A. PEGORETTI

Department of Materials Engineering, University of Trento, Via Mesiano 77, Trento 38050, Italy

Received 29 January 2001; revised 2 November 2001; accepted 2 November 2001

ABSTRACT: Nonelastic deformation of semicrystalline poly(butylene terephtalate) (PBT) was investigated by calorimetric measurements and strain-recovery tests. Differential scanning calorimetry on PBT specimens deformed both below and above their glass-transition temperature ($T_g \approx 50$ °C) showed the presence of a broad exothermal peak whose area represents the energy released for the nonelastic strain recovery. This energy became more and more pronounced as the strain level increased, and it decreased as the deformation temperature increased, even if a significant contribution was detected on specimens deformed at temperatures much higher than T_g. For two temperature conditions (21 and 100 °C), strain-recovery master curves were built showing the following two distinct deformation components: one recoverable with time and another one irreversible, this latter one arising from relatively low levels of strain. The recoverable component can be erased by heating the material at temperatures much higher than its T_g, close to the onset of the melting process. On the other hand, the irreversible strain component does not recover even if the material is brought close to the onset of the crystals melting. The shift factor for the strain-recovery master curves was compared with the shift factor for the construction of the dynamic storage modulus master curve obtained in the linear viscoelastic regime (small strain). © 2001 John Wiley & Sons, Inc. J Polym Sci Part B: Polym Phys 40: 236–243, 2002

Keywords: nonelastic deformation; strain recovery; semicrystalline polymers; poly(butylene terephthalate); viscoelasticity; polyesters; strain; viscoelastic properties

INTRODUCTION

In amorphous glassy polymers three of the following components of deformation are commonly distinguished: elastic, anelastic, and plastic.[1–13] The elastic strain component recovers instantaneously after sample unloading, whereas both the anelastic and plastic components recover with time, although the former has faster kinetics.[7] Temperature accelerates the strain-recovery processes, and it can be observed that the anelastic strain can be completely erased by heating the sample up to a temperature some 20 °C below the glass-transition temperature (T_g), whereas the plastic one needs heating at least up to T_g.[3,7,8,13] The different nature of the associated molecular motions determines the distinct time intervals for the recovery of the two strain components at temperatures lower than $T_g - 20$ °C.[7,8] According to the molecular model proposed by Perez and coworkers,[14–18] the primary effect of strain in polymer glasses is the nucleation of very localized shear microdomains (SMDs) that are associated with the anelastic deformation. The eventual appearance of plastic deformation is determined by the interaction of two or more SMDs that causes molecular rearrangement and conformational

Correspondence to: A. Pegoretti (E-mail: alessandro.pegoretti@ing.unitn.it)

Journal of Polymer Science: Part B: Polymer Physics, Vol. 40, 236–243 (2002)

DOI 10.1002/polb.10085

changes in the polymer. Substantially similar mechanisms were also described by Oleinik and coworkers.[6,19]

Strain-recovery studies at high levels of deformation on semicrystalline polymers are relatively few.[20–26] In semicrystalline polymers such as poly(ethylene terephthalate) (PET), nylon-6 (PA6), and poly(ethylene-2,6-naphthalene dicarboxylate) (PEN), deformed below T_g to a tensile strain of 20%, two components of nonelastic deformation can still be distinguished, that is, a fast-relaxing component (anelastic) and a slow-relaxing component (plastic).[25,26] Strain recovery of both components is accelerated by increasing temperature, but it is necessary to heat the sample well above T_g to erase completely the plastic deformation. The irreversible component of deformation is practically negligible, with at least up to 20% tensile strain.[25,26]

This work further investigates the nature of large deformations in semicrystalline polymers. Calorimetric measurements on poly(butylene terephthalate) (PBT) samples deformed in uniaxial compression to different strain levels, at temperatures both below and above T_g, were carried out. Strain-recovery master curves for two different levels of strain and two different deformation temperatures, below and above T_g, respectively, were also obtained.

EXPERIMENTAL

Specimen Preparation

Specimens, in the form of cubes (6 × 6 × 6 mm) and rectangular bars (60 × 12 × 6 mm), were machined from injection-molded PBT rectangular test bars (127 × 12 × 6 mm) supplied by Radici Novacips SpA (Villa d'Ogna, Bergamo, Italy). All specimens were treated for 3 h at 190 °C under vacuum and slowly cooled down in an oven to erase any thermal stress and maintain the thermal history.

Differential Scanning Calorimetry (DSC)

DSC measurements were performed by a Mettler DSC-30 calorimeter to determine the T_g, melting point (T_m), and crystallinity degree (X_c) of the material. Measurements were performed on about 20 mg of material, obtained from a central part of the cubic specimens, at a heating rate of 10 °C/min in a nitrogen flux of about 200 mL/min.

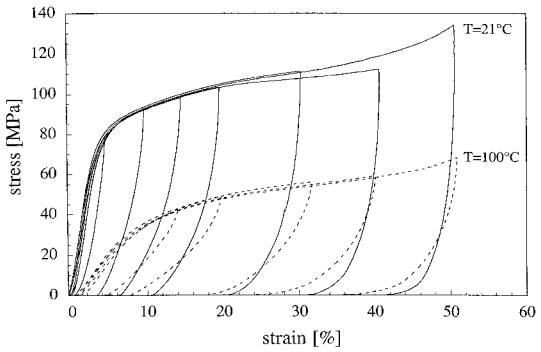

Figure 1. Loading–unloading curves up to various strain levels (5, 14, 20, 30, 40, and 50%) for PBT deformed at two different temperatures below and above T_g: continuous lines (T_{def} = 21 °C) and dashed lines (T_{def} = 100 °C).

For the undeformed material the following results were obtained: $T_g \approx 50$ °C, $T_m \approx 230$ °C, and $X_c \approx 38\%$. The crystallinity percentage was assessed by integrating the normalized area under the endothermal peak and ratioing the heat involved to the reference value of the 100% crystalline polymer, corresponding to 145 J/g.[27] Calorimetric measurements were also performed, under the conditions previously reported, on the materials deformed at various strain levels, ϵ_0, and temperatures, T_{def}.

Deformation and Strain Recovery

Cubic specimens were subjected to uniaxial compression up to various strain levels, ϵ_0, in the range between 5 and 69% by an Instron universal testing machine model 4502, equipped with an Instron thermostatic chamber model 3119. The loading–unloading cycles were performed at a constant crosshead speed of 1 mm/min at various temperatures below and above the T_g. Sample strain during a loading–unloading cycle was detected with an Instron strain gauge extensometer model 2620 fixed to the compression plates. Stress-strain curves for loading–unloading cycles at various strain levels and two different temperatures (21 and 100 °C) are reported in Figure 1. For each deformation temperature and strain level, strain-recovery tests after unloading were performed at various temperatures by monitoring the residual strain, ϵ_{res}, of samples positioned in a small thermostatic chamber (Minimat by Polymer Laboratories, Ltd., U.K.). Specimen displacement during recovery was detected by using a digital micrometer comparator. The recovery tem-

perature range spanned from 21 to 90 °C for the samples deformed at 21 °C and from 100 to 190 °C for those deformed at 100 °C. For each given recovery temperature a different specimen was used for the recovery test. Each specimen was positioned in the thermostatic chamber about 30 s after unloading, and a fixed thermostating period of 3 min was adopted before starting strain-recovery measurements.

Dynamic Mechanical Thermal Analysis (DMTA)

Rectangular bars were used to perform DMTA measurements by a Polymer Laboratories MkII dynamic thermal analyser in a single cantilever configuration. Tests were performed by scanning the temperature in the range from 0 to 180 °C at a heating rate of 0.4 °C min^{-1} at six different frequencies, that is, 0.3, 1, 3, 10, 30, and 50 Hz. A peak-to-peak displacement of 64 μm was set to apply a small strain amplitude (in any case lower than 0.12%) in the linear viscoelastic region.

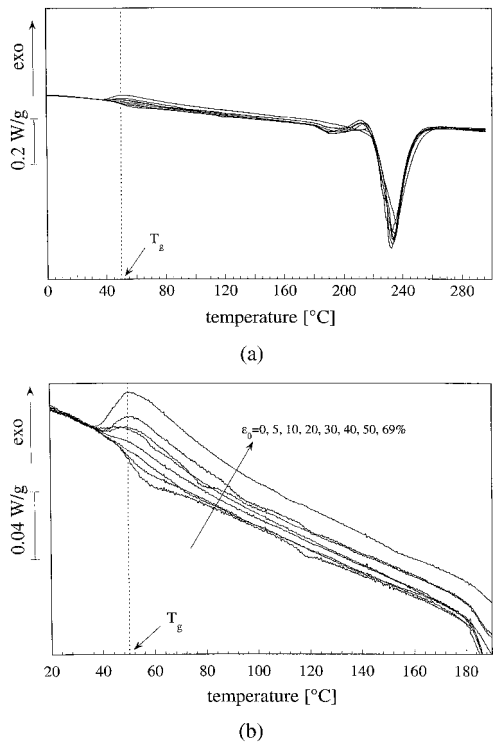

Figure 2. (a) DSC traces of PBT samples deformed at T_{def} = 21 °C (i.e., below T_g) at various applied strains and (b) magnification of Figure 2(a).

RESULTS AND DISCUSSION

DSC

DSC analysis of the undeformed material, and of those deformed below T_g, provided the thermograms depicted in Figures 2(a,b), this latter one being a magnification of Figure 2(a) in the temperature range between 20 and 190 °C.

For the deformed samples, the results clearly show the presence of a broad exothermal peak (or plateau) that becomes more and more pronounced as the strain level increases. This peak ranges from temperatures somewhat higher than the deformation temperature (T_{def} = 21 °C) up to temperatures involved in recrystallization and melting processes. Many researchers[1–6,9,12,13,22,25,28,29] have found in DSC traces of highly deformed polymers an exothermal peak or plateau that for glassy polymers extends typically from the temperature of deformation up to the T_g or little above.[3,4,9,12,13] The area under the peak, ΔH_{exo}, has been attributed to the energy released for the nonelastic strain recovery.[3,4,9,12,13,22,25] The results here obtained suggest that the reversible component of the deformation is associated with relaxation processes that require temperatures well above T_g to be activated. In other semicrystalline polymers (PA6, PET, and PEN), these relaxation processes have been attributed[25,26] to a mobility gradient within the interphase between the crystalline domains and the amorphous component of the polymer.[30]

DSC traces obtained on samples deformed at 100 °C (i.e., ca. 50 °C above T_g) are illustrated in Figures 3(a,b), this latter one being a magnification of Figure 3(a) in the temperature range between 20 and 180 °C. The diagrams still show a broad exothermal peak that becomes more and more pronounced as the applied strain increases. For any applied strain level examined, the peak initiates from about T_g and extends up to temperatures involved in the onset of the melting process. More precisely, the area under the peak shows a minor contribution between T_g and T_{def} and a second major contribution at temperatures higher than T_{def}. For each considered strain level and deformation temperature, the area under the exothermal peak, ΔH_{exo}, was evaluated by integrating the area enclosed between the traces obtained for the undeformed and deformed material between the temperature limits corresponding to the onset of the peak up to about 180 °C. Values of ΔH_{exo} are illustrated in Figure 4 as a function of the applied strain for the two deformation tem-

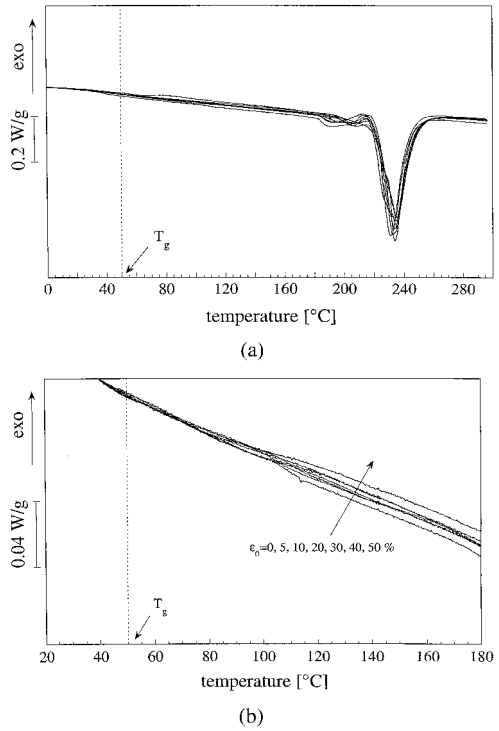

Figure 3. (a) DSC traces of PBT samples deformed at T_{def} = 100 °C (i.e., above T_g) at various applied strains and (b) magnification of Figure 3(a).

peratures considered. For T_{def} = 100 °C, it is interesting to observe the appearance of a considerable deformational component that is recoverable at temperatures much higher than both T_g and T_{def}. This component increases by increasing the total applied strain, although at any strain level, ΔH_{exo} for the samples deformed at T_{def} = 100 °C is lower than for the samples deformed at room temperature. The reversible nature of the energy stored in the materials deformed both below and above T_g, and represented by ΔH_{exo}, is confirmed by the fact that at any considered applied strain a thermal treatment at 190 °C for 30 min provides the restoration of the original DSC trace corresponding to the undeformed material. Contrary to the behavior of glassy polymers,[3] an exothermic peak for specimens deformed at a temperature well above T_g indicates that the reversible component of deformation associated with this peak involves necessarily the crystalline part of the polymer and/or the interphase between the crystalline domains and the amorphous part of the polymer. As shown by DSC traces reported in Figure 5, samples compressed up to a strain of 69% at different temperatures between 20 and 160 °C showed that ΔH_{exo} decreases by increasing T_{def}. On the other hand, the temperature, T_{exo}, at which the major contribution to the exothermal peak initiates, increases by increasing T_{def}. These results are also displayed in Figure 6.

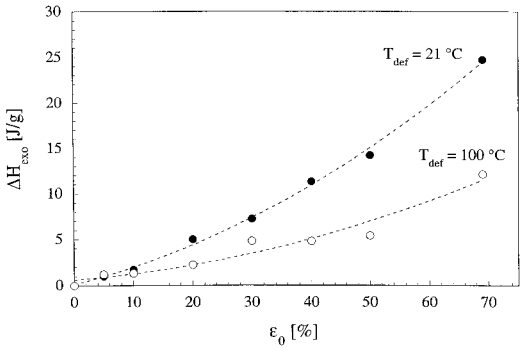

Figure 4. Area under the exothermal peak in the DSC traces, ΔH_{exo}, versus applied strain for T_{def} below (●, T_{def} = 21 °C) and above (○, T_{def} = 100 °C) the T_g.

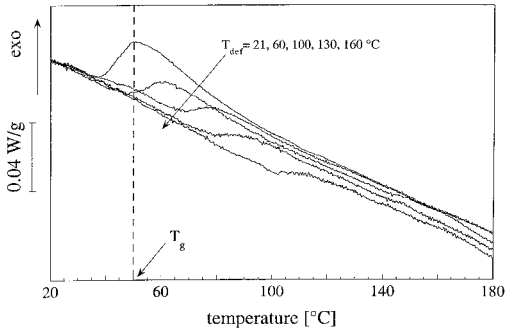

Figure 5. DSC traces of PBT samples deformed at various deformation temperatures (T_{def} = 21, 60, 100, 130, and 160 °C) up to ε_0 = 69%.

Strain Recovery

Strain-recovery tests confirmed the presence of a recoverable component of deformation and showed the presence of an irreversible contribution that initiates from relatively low levels of strain (ca. 5–10%) and increases with the applied strain. This component remains frozen in the material after a thermal treatment at 190 °C for 30 min, as shown in Figure 7 for samples deformed at room temperature at different levels of strain.

Strain-recovery data at different temperatures, such as those reported in Figure 8, show the thermomechanically activated nature of strain recovery as it occurs for fully amorphous glassy polymers[7,8] and other semicrystalline poly-

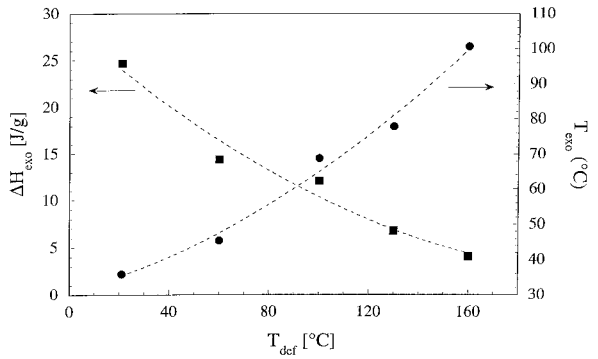

Figure 6. ΔH_{exo} and T_{exo} as a function of T_{def} for ε_0 = 69%.

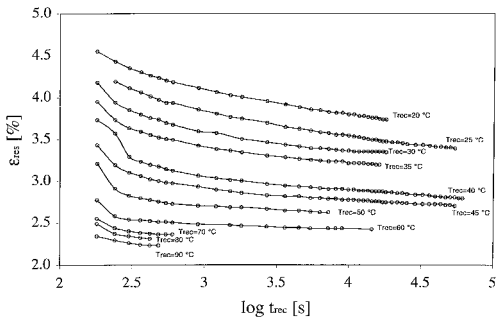

Figure 8. Strain-recovery data at various recovery temperatures, T_{rec}, for ε_0 = 14% and T_{def} = 21 °C.

mers.[25,26] Strain-recovery master curves were determined both for T_{def} = 21 °C at two strain levels, 14 and 30%, and for T_{def} = 100 °C at 30% strain. Each recovery master curve was built by shifting on the timescale the curves of residual strain versus time obtained at different recovery temperatures, following a time-temperature reduction scheme.[7,8,25,26] In the shift procedure, the data concerning times lower than 5.3 min, that is, $\log(t_{rec})$ = 2.5 s (see Fig. 8), were neglected to ensure a better isothermal regime at the various recovery temperatures. Strain-recovery master curves referred to as T_{ref} = 21 °C are reported in Figure 9 for samples deformed at T_{def} = 21 °C up to two different levels of the applied strain, 14 and 30%, respectively. In the same figure the master curve referred to as T_{ref} = 100 °C is reported for samples deformed at T_{def} = 100 °C and at 30% strain. The relative position of the curves a) and b) corresponding to the two different strains (T_{def} = 21 °C) confirms the presence of an irreversible component of deformation, represented by the plateau level at long times, that increases by increasing the applied strain. The master curves b) and c), relative to the two different deformation temperatures (at ϵ_0 = 30%), although referred to as different temperatures, seem to converge at very long times in agreement with the fact that the irreversible component of the deformation is the same in the two cases. The shift factors obtained for various recovery master curves are reported in Figure 10 as a function of the inverse value of the absolute temperature. The two shift factors corresponding to the recovery processes of samples deformed at the same temperature (T_{def} = 21 °C) show a similar trend regardless of the level of the applied strain (14 and 30%, respectively). This seems to indicate that the nature of the thermally activated mechanisms of strain recovery should be the same in the two cases. By contrast, the shift factors corresponding to the recovery of samples deformed to

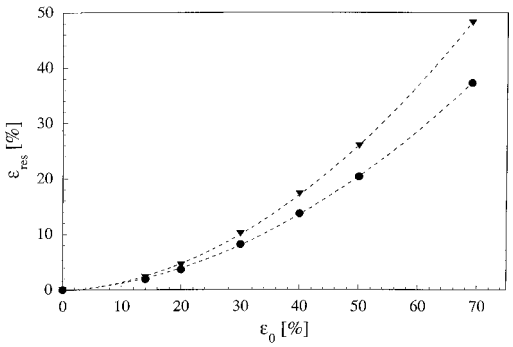

Figure 7. Residual strain, ε_{res}, versus total applied strain, ε_0, at T_{def} = 21 °C after thermal treatments at 90 °C for 1 h (▼) and at 190 °C for 30 min (●).

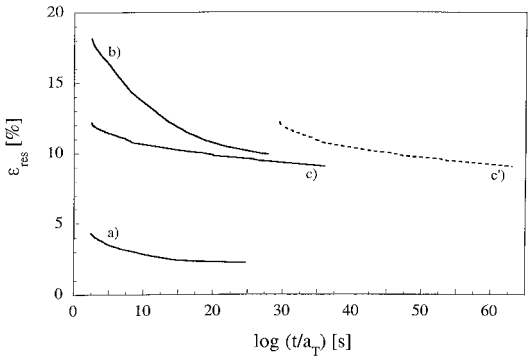

Figure 9. Strain-recovery master curves for PBT samples: a) deformed at T_{def} = 21 °C up to ε_0 = 14% (T_{ref} = 21 °C), b) deformed at T_{def} = 21 °C up to ε_0 = 30% (T_{ref} = 21 °C), c) deformed at T_{def} = 100 °C up to ε_0 = 30% (T_{ref} = 100 °C), and c′) deformed at T_{def} = 100 °C up to ε_0 = 30% (T_{ref} = 21 °C).

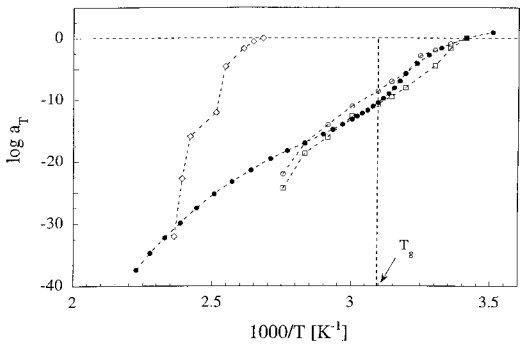

Figure 10. Comparison among shift factors for the construction of master curves: (○) strain recovery at ε_0 = 14%, T_{def} = 21 °C, T_{ref} = 21 °C; (□) strain recovery at ε_0 = 30%, T_{def} = 21 °C, T_{ref} = 21 °C; (◇) strain recovery at ε_0 = 30%, T_{def} = 100 °C, T_{ref} = 100 °C; and (●) dynamic storage modulus.

the same strain level (30%) at two different deformation temperatures show a quite different behavior within the respective temperature ranges explored. Moreover, by considering the shift factors reported in Figure 10, it is possible to observe that the curve c) of Figure 9 could be referred to as T_{ref} = 21 °C through a horizontal shift that can be estimated as equal to about 27 decades. The result of this shifting procedure is represented by the dotted curve c′) of Figure 9 that represents the master curve referred to as 21 °C for the strain recovery of samples deformed at ϵ_0 = 30% at T_{def} = 100 °C. There is no superposition between curves b) and c′) of Figure 9, thus revealing that different deformation/recovery mechanisms are active at the two deformation temperatures considered (i.e., 21 and 100 °C).

Experimental data of the storage and loss moduli, E' and E'', were obtained by DMTA at various test frequencies, f, in the temperature range from 0 to 180 °C. The cross plots of the experimental curves (drawn as a function of temperature) allowed the construction of a series of isothermal curves of E' as a function of test frequency[31] in the experimental range 0.3–30 Hz as represented in Figure 11(a). These isothermal curves were then horizontally shifted to best superposition according to a frequency-temperature superposition approach to obtain a master curve of dynamic storage modulus E' at the reference temperature of 21 °C [see Fig. 11(b)]. The validity of this approach to PBT that could suffer some possible thermorheological complexity because of its semicrystalline nature can be checked by using the Cole–Cole model.[32] According to this model, first derived to discuss dielectric results,[32] the complex modulus, E^*, is described by the following empirical equation:

$$E^*(\omega) = E_u + \frac{E_r - E_u}{1 + (i\omega\tau_0)^{1-\alpha}} \quad (1)$$

where E^* is the complex modulus, ω is the angular frequency ($\omega = 2\pi f$), E_u and E_r are the unrelaxed and relaxed moduli, respectively, τ_0 is the average relaxation time, and α is a parameter between 0 and 1 related to the width of the distribution of the relaxation times. Following an approach recently used to treat dynamic mechanical data of high-density polyethylene,[33] the real component of the complex modulus of eq 1 can be written as

$$E'(\omega) = E_u + \frac{E_r - E_u}{2} \times \left\{1 - \frac{\sinh[(1-\alpha)\ln(\omega\tau_0)]}{\cosh[(1-\alpha)\ln(\omega\tau_0)] + \sin\left(\alpha\frac{\pi}{2}\right)}\right\} \quad (2)$$

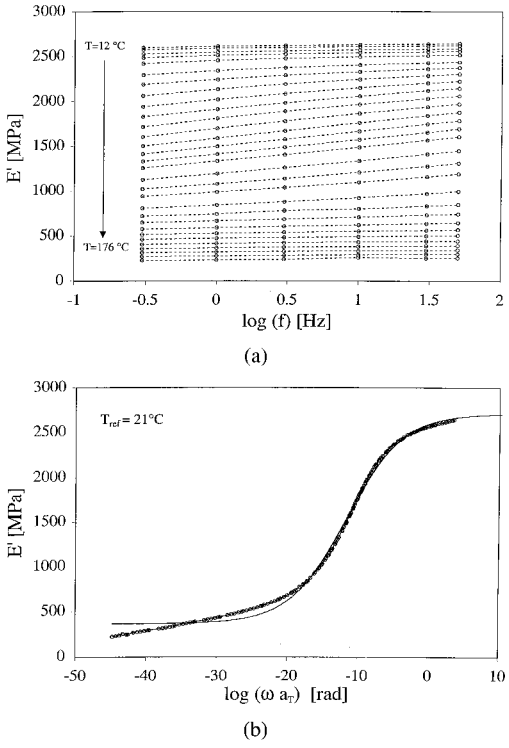

Figure 11. DMTA measurements: a) isothermal storage modulus, E', as a function of test frequency and b) storage modulus master curve referred to as T_{ref} = 21 °C (solid line corresponds to the best fitting curve described in eq 2).

where eq 2 was used to fit data with E_u, E_r, τ_0, and α as adjustable parameters. The best fitting procedure, which was performed on a least-squares minimization basis, provided the following values: E_u = 2709 MPa, E_r = 366 MPa, τ_0 = 4.2 $\times$ 10^{11} s, and α = 0.89076. In Figure 11(b) the fitting curve (solid line) agrees with the master curve data points. Some disagreement appears in the low-frequency regions (data obtained at temperatures higher than 100 °C).

The procedure of frequency-temperature reduction provided an empirical determination of the shift factor for the master curve, a_T, as a function of temperature, which is reported in Figure 10. The similarity between the temperature dependence of the shift factors for both E' and strain-recovery (at T_{def} = 21 °C) master curves confirms that viscoelastic relaxation processes have similar activation energies regardless of the deformation level considered.

The analysis of the kinetics of strain recovery on the basis of the master curves has not allowed a distinction between anelastic (fast-relaxing) and plastic (slow-relaxing) components of deformation as for other semicrystalline polymers.[25,26] Nevertheless, on the basis of the experimental data, the total deformation ϵ_0 is composed by three components, that is, an elastic strain, ϵ_{el}, that recovers instantaneously; a nonelastic reversible component, ϵ_{ner}, that recovers in a lapse of time; and an irreversible component, ϵ_{irr}. To prevent misunderstanding and confusion, the terms "anelastic" and "plastic" are avoided. For the samples deformed at 21 °C to different applied strains, the contributions to the total deformation were evaluated in the following manner: the elastic component was taken as $\epsilon_{el} = \sigma/E_u$, E_u being the unrelaxed modulus, the irreversible component was evaluated as the residual strain after a thermal treatment at 190 °C for 0.5 h, and the nonelastic term, ϵ_{ner}, was verified by the difference $\epsilon_{ner} = \epsilon_0 - \epsilon_{irr}$. Figure 12 shows the strain partitioning among the different contributions with varying applied strain. ϵ_{ner} nucleates immediately and increases by increasing the applied strain flattening at high strain levels, whereas ϵ_{irr} nucleates for strains higher than 6–8%, which corresponds to the macroscopic yield point, and increases more steeply at high levels of the applied strain.

It would be interesting to ascertain if both the nonelastic reversible and irreversible components of strain involve the orientation and/or integrity of the crystalline domains. Evidence of orientation, crystallite texture change, and disentanglement processes have been found to occur in polyethylene and related copolymers during cold-drawing in uniaxial tension[34,35] as well as different crystallographic deformation mechanisms in high-density polyethylene in plane-strain compression.[36,37] Some of these mechanisms could also be operative in PBT, and X-ray diffraction analysis of the deformed materials could provide information on possible deformation mechanisms involving orientations and structural changes of the crystalline domains. This work is in progress.

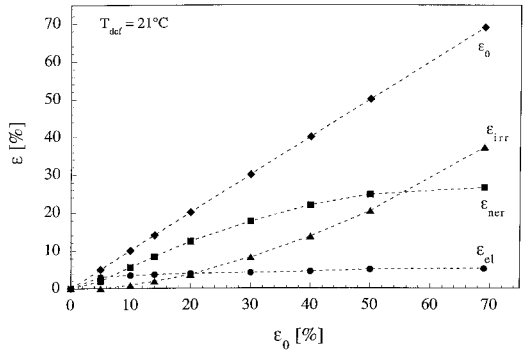

Figure 12. Strain partitioning among elastic, ε_{el} (○), nonelastic reversible, ε_{ner} (■), and irreversible, ε_{irr} (▲), contributions versus applied strain, ε_0 (◆), for PBT samples deformed at 21 °C (i.e., below T_g).

CONCLUSIONS

In semicrystalline PBT, deformed both below and above T_g, DSC experiments revealed a nonelastic deformation component that recovers with time and can be erased completely only by heating the deformed specimens up to the onset of the melting process. The amount of released energy, detected as an exothermal peak in DSC analysis, becomes more and more pronounced as the strain level increases, and it decreases as the deformation temperature increases. A significant energy contribution is detected even for specimens deformed at temperatures much higher than T_g.

Strain-recovery master curves at different levels of initial deformation and different deformation temperatures were constructed from strain-recovery data obtained at various recovery temperatures on the basis of a time-temperature superposition procedure. The analysis of the associated shift factors seems to indicate that different deformation/

recovery mechanisms are active at the two deformation temperatures considered (i.e., 21 and 100 °C). Contrary to fully amorphous polymers, strain-recovery master curves obtained on samples deformed at 21 and 100 °C revealed that a clear distinction between anelastic and plastic deformation, referred as fast- and slow-relaxing components, respectively, is uncertain and questionable. Moreover, an irreversible component of deformation appears from relatively low levels of strain. For all these reasons, the terms anelastic and plastic, applied to the data obtained in this article, appear to be confusing and misleading. As a consequence, the contribution of elastic, ϵ_{el}, nonelastic reversible, ϵ_{ner}, and irreversible ϵ_{irr}, components to the total deformation, ϵ_0, was envisaged and quantitatively established.

This work was partially supported by Ministero dell'Università e della Ricerca Scientifica e Tecnologica (MURST), Rome. Radici Novacips SpA (Villa D'Ogna, Bergamo, Italy) is acknowledged for the provision of the materials. The authors thank A.Guardini for his contribution to the experimental work.

REFERENCES AND NOTES

1. Oleinik, E. F. Adv Polym Sci 1986, 80, 49–99.
2. Oleinik, E. F. Prog Colloid Polym Sci 1989, 80, 140–150.
3. Oleinik, E. F. In High Performance Polymers: Structure, Properties, Composites, Fibers; Baer, E.; Moet, A., Eds.; Hanser: Munich, 1991; pp 79–102.
4. Salamantina, O. B.; Rudnev, S. N.; Voenniy, V. V.; Oleinik, E. F. J Therm Anal 1992, 38, 1271–1281.
5. Oleinik, E. F.; Salamantina, O. B.; Rudnesv, S. N.; Shenogin, S. V. Polym Sci 1993, 35, 1532–1558.
6. Salamantina, O. B.; Hone, G. W. H.; Rudnev, S. N.; Oleinik, E. F. Thermochim Acta 1994, 247, 1–18.
7. Quinson, R.; Perez, J.; Rink, M.; Pavan, A. J Mater Sci 1996, 31, 4387–4394.
8. David, R.; Quinson, R.; Gauthier, C.; Perez, J. Polym Eng Sci 1997, 3, 1633–1640.
9. Hasan, O. A.; Boyce, M. C. Polymer 1993, 34, 5085–5092.
10. Hasan, O. A.; Boyce, M. C.; Li, X. S.; Berko, S. J Polym Sci Part B: Polym Phys 1993, 31, 185–197.
11. Hasan, O. A.; Boyce, M. C. Polym Eng Sci 1995, 35, 331–344.
12. Chang, B. T.; Li, J. C. M. Polym Eng Sci 1988, 28, 1198–1202.
13. Kung, T. M.; Li, J. C. M. J Mater Sci 1987, 22, 3620–3630.
14. Perez, J. Physique et Mecanique des Polymers Amorphes; Lavoisier: Paris, 1992.
15. Mangion, M. B. M.; Cavaille, J. Y.; Perez, J. Philos Mag A 1992, 66, 773–796.
16. Perez, J.; Cavaille, J. Y.; Etienne, S.; Fouquet, F. J Phys (Paris) 1980, 41, C8–850.
17. Cavaille, J. Y.; Perez, J. Johari, G. P. J Non-Cryst Solids 1991, 131–133, 935–941.
18. Gauthier, C.; Pelletier, J. M.; David, L.; Vigier, G.; Perez, J. J Non-Cryst Solids 2000, 274, 181–187.
19. Oleinik, E. F. Polym Sci USSR 1993, 35(11), 1819–1849.
20. Park, J. B.; Uhlmann, D. R. J Appl Phys 1970, 41(7), 2928–2935.
21. Park, J. B.; Uhlmann, D. R. J Appl Phys 1971, 42(10), 3800–3805.
22. Park, J. B.; Uhlmann, D. R. J Appl Phys 1973, 44(1), 201–206.
23. Tanaka, N. J Therm Anal 1996, 46, 1021–1031.
24. Charoensirisomboon, P.; Saito, H.; Inoue, T.; Oishi, Y.; Mori, K. Polymer 1998, 39(11), 2089–2093.
25. Pegoretti, A.; Guardini, A.; Migliaresi, C.; Ricco, T. Polymer 2000, 41, 1857–1864.
26. Pegoretti, A.; Guardini, A.; Migliaresi, C.; Ricco, T. J Appl Polym Sci 2000, 78, 1664–1770.
27. Van Krevelen, D. W. Properties of Polymers; Elsevier: Amsterdam, 1990; Chapter 5, p 121.
28. Berens, A. R.; Hodge, I. M. Macromolecules 1982, 15, 756–761.
29. Bawens-Crowet, C.; Bawens, J. C. Polymer 1987, 28, 1863–1868.
30. Struik, L. C. E. Physical Aging in Amorphous Polymers and Other Materials; Elsevier: Amsterdam, 1978; pp 55–56.
31. Ricco, T.; Pegoretti, A. Polym Eng Sci 2000, 40(10), 2227–2231.
32. Cole, R. H.; Cole, K. S. J Chem Phys 1941, 9, 341.
33. Mano, J. F.; Sousa, R. A.; Reis, R. L.; Cunha, A. M.; Bevis, M. J. Polymer 2001, 42, 6187–6198.
34. Hiss, R.; Hobeika, S.; Lynn, C.; Strobl, G. Macromolecules 1999, 32, 4390–4403.
35. Hobeika, S.; Men, Y.; Strobl, G. Macromolecules 2000, 33, 1827–1833.
36. Bartzak, Z.; Argon, A. S.; Cohen, R. E. Macromolecules 1992, 25, 5036–5053.
37. Galeski, A.; Bartzak, Z.; Argon, A. S.; Cohen, R. E. Macromolecules 1992, 25, 5705–5718.